Control of Electron-Transfer and DNA Binding Properties by the Tolyl Spacer Group in Viologen Linked Acridines

Joshy Joseph, Nadukkudy V. Eldho,† and Danaboyina Ramaiah*

Photosciences and Photonics Division, Regional Research Laboratory (CSIR), Trivandrum, India 695 019

Received: October 18, 2002; In Final Form: February 15, 2003

Novel water soluble viologen and pyridinium linked tolylacridines **1a,b** and **2a,b** were synthesized and their photophysical and DNA binding properties including the photoinduced electron-transfer reactions were investigated. When compared to the cases of the model tolylacridines **3a,b** and the pyridinium linked derivatives **2a,b**, the singlet excited states of **1a** and **1b** were efficiently quenched in water and methanol. Intramolecular quenching rate constants (k_{ET}) calculated in water are found to be 1.2×10^{10} and 8.8×10^{10} s^{-1} for **1a** and **1b** and 1.4×10^{8} and 0.9×10^{8} s^{-1} for **2a** and **2b**, respectively, suggesting thereby that the viologen moiety quenches the fluorescence of the acridine chromophore efficiently when compared to the case of the pyridinium moiety. From the intermolecular electron-transfer studies, it was observed that the singlet and triplet excited states of the acridine chromophore are capable of donating an electron to the viologen moiety. DNA binding studies indicated that the *p*-tolylacridine derivatives **1a** and **2a** exhibit strong binding to DNA with binding constants of 1.0×10^{5} and 3.3×10^{5} M^{-1}, respectively, whereas the *o*-tolylacridine derivatives **1b** and **2b** showed negligible affinity for DNA. The rate constants for the static quenching of **1a** and **2a** by DNA (k_{DNA}) are found to be 7×10^{9} and 3×10^{9} s^{-1}, respectively, indicating that **1a** is an efficient DNA oxidizing agent. Nanosecond laser flash photolysis studies of these systems in aqueous solutions did not show any transients. However, in the presence of DNA, **1a** gave transient absorption due to the reduced methyl viologen radical cation. These results demonstrate that the tolyl spacer group in these systems constitutes an interesting variation which controls both the electron transfer and DNA binding properties, and hence, such molecules and derivatives thereof can have potential application as probes for nucleic acids and as DNA cleaving agents.

Introduction

Design of molecules targeting nucleic acids is an active area of research. Several classes of molecules, which induce DNA modifications by various mechanisms, have been reported in the literature.[1−13] Among these, the photoactivated DNA cleaving agents show some advantages, such as (i) better control of the reaction trigger, (ii) selectivity of the reaction center by adjusting the wavelength of irradiation, and (iii) the ability to control light, which helps to minimize the side reactions and thus leads to a better understanding of the reaction mechanism. By absorption of light, these reagents are known to modify DNA through different mechanisms, including the electron-transfer reaction, generation of diffusible intermediates, and H-atom abstraction.[14] In the latter two processes, selectivity of the DNA cleavage is rather difficult to attain, as these reactions are generally nonspecific, while the former mechanism is shown to have base selectivity. The major challenges associated with the DNA cleavage through the electron-transfer mechanism include (i) efficiency of the DNA oxidation and (ii) selectivity of the DNA cleavage. The inefficiency associated with such reactions is the fast recombination of the charge separated species, such as the oxidized base and the reduced agent. To improve the efficiency of the DNA cleavage through the electron-transfer mechanism, a cosensitization approach has been introduced recently.[15] In this approach, the photoactivated DNA cleaving agent comprises a sensitizer, which is either free or covalently linked to a cosensitizer moiety and wherein both these moieties are capable of binding to DNA through noncovalent interactions.[15−17]

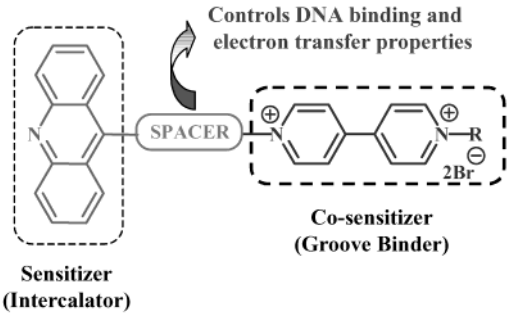

Figure 1. Schematic representation of the strategy adopted for the design of photoactivated DNA cleaving agents.

With the objective of developing efficient photoactivated DNA cleaving agents, which function through the electron-transfer mechanism,[18] we have designed bifunctional derivatives (Figure 1), where an intercalator (acridine) is linked to a groove binder (viologen) through a spacer group. The intercalator is so chosen that it can act as a sensitizer, which upon excitation can transfer an electron to the viologen moiety, leading to the radical cation of acridine and the radical cation of viologen. The radical cation of acridine, once formed, can oxidize DNA bases with a preference to guanine and thus can initiate oxidative modification of DNA. The challenging difficulties involved are

* To whom correspondence should be addressed. Telephone: +91 471 2515362. Fax: +91 471 2490186 or +91 471 2491712. E-mail: d_ramaiah@rediffmail.com or rama@csrrltrd.ren.nic.in.

† Current address: Laboratory of Membrane Biochemistry and Biophysics, NIH, Baltimore, MD 20852, USA.

10.1021/jp027248q CCC: $25.00
Published on Web 04/12/2003

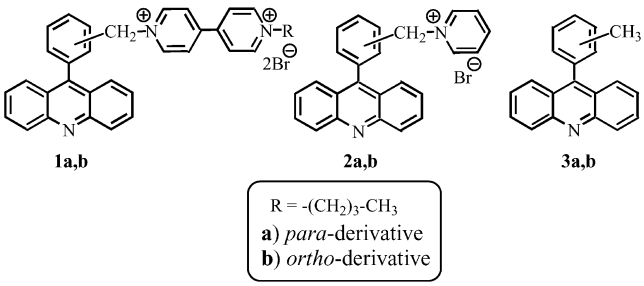

Figure 2. Structures of the tolylacridine derivatives **1a,b**, **2a,b**, and **3a,b** under investigation.

to get a control over the DNA binding and photoinduced electron-transfer reaction to produce long-lived charge-separated species, which regulate the efficiency of the DNA cleavage through this mechanism.

Another objective of our investigation is to examine the effect of the spacer group on the DNA intercalating property of the acridine moiety, which in turn can control the efficiency of the DNA photocleavage. Here we describe our results on the photophysical and DNA binding properties, including intra- and intermolecular electron-transfer reactions of a few viologen and pyridinium linked tolylacridine derivatives (Figure 2). These results demonstrate that the tolyl spacer group constitutes an interesting variation and plays a major role in controlling the photophysical and DNA binding properties of these novel molecules.

Experimental Section

General Techniques. The equipment and procedure for melting point determination and spectral recordings are described in earlier publications.[19,20] The fluorescence quantum yields were determined by using optically matching solutions. 9-Aminoacridine in methanol ($\Phi_f = 0.99$) was used as the standard.[21] The fluorescence lifetimes were measured on an Edinburgh FL900CD single photon counting system. Fluorescence lifetimes were determined by convoluting the instrumental function with a mono- or biexponential decay and minimizing the χ^2 values of the fit to 1 ± 0.1. Laser flash photolysis experiments were carried out in an Applied Photophysics model LKS-20 laser kinetic spectrometer using the third harmonic (355 nm) of a Quanta Ray GCR-12 series pulsed Nd:YAG laser. The DNA binding studies were carried out in 10 mM phosphate buffer containing 2, 50, and 100 mM NaCl. The DNA binding affinities were calculated according to the method of McGhee and von Hippel by using the data points of the Scatchard plot.[22−24] The spectroscopic measurements in water were carried out at pH 9 to avoid the protonation of the excited state of acridine. Petroleum ether used was the fraction with bp = 60−80 °C.

Materials. 4,4′-Bipyridine and methyl viologen dichloride hydrate (98%) were obtained from Aldrich and used as received. A solution of calf thymus DNA (Pharmacia Biotech, USA) was sonicated for 1 h and filtered through a 0.45 μM Millipore filter. The concentrations of DNA solutions were determined by using the average value of 6600 M^{-1} cm^{-1} for the extinction coefficient of a single nucleotide at 260 nm.[25] 1-Butyl-4,4′-bipyridinium bromide was obtained in 95% yield by the reaction of 4,4′-bipyridine with 1-bromobutane in the molar ratio 3:1 in dry acetonitrile.[26] The synthesis of 9-(4-methylphenyl)acridine (**3a**), mp 188−189 °C (lit. mp 189 °C),[27] and 9-(2-methylphenyl)-acridine (**3b**), mp 212−213 °C (lit. mp 214 °C),[27,28] was achieved as per the reported procedures.

Synthesis of 9-(4-Bromomethylphenyl)acridine and 9-(2-Bromomethylphenyl)acridine. A solution of 9-(4-methylphenyl)-acridine (**3a**, 1 mmol), *N*-bromosuccinimide (NBS, 1 mmol), and benzoyl peroxide (20 mg) in dry CCl_4 (20 mL) was refluxed for 8 h. The reaction mixture was cooled and filtered. The filtrate was concentrated to give a residue, which was chromatographed over a silica gel column. Elution of the column with a mixture (1:4) of ethyl acetate and petroleum ether gave 9-(4-bromomethylphenyl)acridine in 60% yield, mp 203−204 °C: ^{1}H NMR ($CDCl_3$, 300 MHz) δ 4.7 (2H, s), 7.3−8.05 (8H, m), 8.25−8.50 (4H, m); ^{13}C NMR ($CDCl_3$, 75 MHz) δ 148.60, 146.28, 137.95, 136.04, 130.85, 129.96, 129.54, 129.06, 126.52, 125.69, 125.69, 124.92, 32.88. Exact mol wt calcd for $C_{20}H_{15}NBr$ $(M + H)^+$: 348.0388. Found: 348.0384 (high-resolution mass spectrometry).

Similar reaction of 9-(2-methylphenyl)acridine (**3b)** with NBS in dry CCl_4 in the presence of benzoyl peroxide yielded 9-(2-bromomethylphenyl)acridine in 56% yield, mp 136−137 °C: ^{1}H NMR ($CDCl_3$, 300 MHz) δ 4.05 (2H, s), 7.10−7.90 (10H, m), 8.15−8.45 (2H, m); ^{13}C NMR ($CDCl_3$, 75 MHz) δ 148.46, 144.04, 136.49, 135.30, 130.62, 129.75, 129.54, 129.07, 128.26, 126.23, 125.63, 124.96, 30.34. Exact mol wt calcd for $C_{20}H_{15}NBr$ $(M + H)^+$: 348.0388. Found: 348.0394 (high-resolution mass spectrometry).

*Synthesis of the Viologen Linked Tolylacridines **1a** and **1b**.* A solution of 9-(4-bromomethylphenyl)acridine (1 mmol) and 1-butyl-4,4′-bipyridinium bromide (2 mmol) in dry acetonitrile (30 mL) was stirred at 30 °C for 12 h. The precipitated solid was filtered and washed with dry acetonitrile and dichloromethane to remove the unreacted starting materials. The solid was further purified by Soxhlet extraction with dichloromethane and recrystallization from a mixture (4:1) of ethyl acetate and acetonitrile to give 77% of **1a**, mp 268−269 °C: ^{1}H NMR (DMSO-d_6, 300 MHz) δ 0.85−1.05 (3H, t, $J = 2.89$ Hz), 1.15−1.55 (2H, m), 1.80−2.20 (2H, m), 4.70−4.90 (2H, t, $J = 2.80$ Hz), 6.3 (2H, s), 7.50−8.40 (12H, m), 8.75−9.05 (4H, m), 9.42−9.60 (2H, m), 9.70−9.85 (2H, m); ^{13}C NMR (DMSO-d_6, 75 MHz) δ 149.23, 1483.61, 147.74, 146.19, 146.00, 145.76, 136.21, 134.42, 131.09, 130.64, 129.36, 128.94, 127.26, 126.79, 126.38, 126.21, 124.23, 63.87, 60.64, 32.70, 18.77, 13.33; MS *m*/*z* 561 (M^+Br^-, 5), 481 (M^+, 100), 424 (10). Anal. Calcd for $C_{34}H_{31}Br_2N_3$: C, 63.66; H, 4.87; N, 6.55. Found: C, 63.81; H, 5.09; N, 6.42.

Similar reaction of 9-(2-bromomethylphenyl)acridine (1 mmol) with 1-butyl-4,4′-bipyridinium bromide (2 mmol) in dry acetonitrile and purification as in the earlier case gave **1b** in 75% yield, mp 224−225 °C: ^{1}H NMR (DMSO-d_6, 300 MHz) δ 0.80−1.00 (3H, t, $J = 2.89$ Hz), 1.05−1.50 (2H, m), 1.70−2.10 (2H, m), 4.65−4.90 (2H, t, $J = 2.85$ Hz), 5.60 (2H, s), 7.15−8.70 (16H, m), 9.30−9.55 (4H, m); ^{13}C NMR (DMSO-d_6, 75 MHz) δ 148.50, 147.80, 145.82, 145.27, 142.77, 135.64, 132.08, 131.90, 131.36, 130.55, 130.44, 129.98, 129.47, 127.08, 126.68, 126.49, 125.95, 125.34, 124.24, 62.02, 60.64, 32.68, 18.78, 13.35; MS *m*/*z* 561 (M^+Br^-, 7), 481 (M^+, 100), 424 (7). Anal. Calcd for $C_{34}H_{31}Br_2N_3$: C, 63.66; H, 4.87; N, 6.55. Found: C, 63.69; H, 5.06; N, 6.46.

*Synthesis of the Pyridinium Linked Tolylacridines **2a** and **2b**.* A solution of 9-(4-bromomethylphenyl)acridine (1 mmol) and dry pyridine (2 mmol) in dry acetonitrile (30 mL) was stirred at 30 °C for 12 h. The precipitated solid was filtered and washed with dry acetonitrile and dichloromethane to remove the unreacted starting materials. The solid was further purified by Soxhlet extraction with dichloromethane and recrystallization from a mixture of ethyl acetate and acetonitrile (4:1) to give **2a**

in 87% yield, mp 270−272 °C: ^{1}H NMR (DMSO-d_6, 300 MHz) δ 6.05 (2H, s), 7.55−7.60 (6H, m), 7.78−7.86 (4H, m), 8.20−8.25 (4H, m), 8.67−8.72 (H, t, J = 5.7 Hz), 9.31−9.33 (2H, d, J = 5.6 Hz); ^{13}C NMR (DMSO-d_6, 75 MHz) δ 148.63, 146.67, 145.56, 135.21, 134.90, 131.12, 131.623, 130.90, 129.85, 129.55, 129.13, 126.83, 126.65, 124.72, 63.58. Exact mol wt calcd for $C_{25}H_{19}N2$ (M^+): 347.1548. Found: 347.1546 (high-resolution mass spectrometry). Anal. Calcd for $C_{25}H_{19}BrN_2$: C, 70.26; H, 4.48; N, 6.56. Found: C, 70.06; H, 4.55; N, 6.61.

Similar reaction of 9-(2-bromomethylphenyl)acridine (1 mmol) with dry pyridine (2 mmol) in dry acetonitrile and purification as in the earlier case gave **2b** in 83% yield, mp 245−246 °C: ^{1}H NMR (DMSO-d_6, 300 MHz) δ 5.39 (2H, s), 7.16−7.19 (2H, d, J = 8.6 Hz), 7.41−7.57 (5H, m), 7.79−7.85 (5H, m), 8.1−8.22 (5H, m); ^{13}C NMR (DMSO-d_6, 75 MHz) δ 148.58, 147.40, 145.98, 142.47, 135.54, 132.24, 131.36, 130.24, 129.98, 129.81, 127.36, 126.95, 126.62, 126.01, 125.45, 123.52, 61.01. Exact mol wt calcd for $C_{25}H_{19}N2$ (M^+): 347.1548. Found: 347.1551 (high-resolution mass spectrometry). Anal. Calcd for $C_{25}H_{19}BrN_2$: C, 70.26; H, 4.48; N, 6.56. Found: C, 70.34; H, 4.50; N, 6.67.

Cyclic Voltammetry. The cyclic voltammograms were recorded on a BAS CV-50W voltammetric analyzer. A glassy carbon working electrode was used along with platinum auxiliary and Ag/AgCl (3 M NaCl) reference electrodes. The redox potentials obtained were calibrated using ferrocene as an internal standard. The potentials were measured in dry acetonitrile, which contained 0.1 M tetrabutylammonium tetrafluoroborate as the supporting electrolyte. Samples were degassed for 20 min before recording the voltammogram. The sweep rate used was 100 mV/s. Square wave techniques were used to get the half-wave potentials under similar conditions. The measured oxidation potential of **3a** was found to be 1.6 V vs SCE while 1-ethylpyridinium bromide and methyl viologen exhibited reduction potentials of −1.34 and −0.45 V vs SCE, respectively.[29,30]

Free Energy Calculations. The free energy of the electron-transfer reaction (ΔG_{el}) from the singlet/triplet excited states of acridine to the acceptor molecules was calculated using the Rehm−Weller equation (eq 1)[31,32]

$$\Delta G_{el} = E^{\circ}_{(D)} - E^{\circ}_{(A)} - E_{(0,0)} - \frac{e^2}{2}\left(\frac{1}{r_D} + \frac{1}{r_A}\right)\left(\frac{1}{37} - \frac{1}{\epsilon_s}\right) - \frac{e^2}{\epsilon_s d_{cc}} \quad (1)$$

where $E^{\circ}_{(D)}$ is the oxidation potential of the donor (acridine), $E^{\circ}_{(A)}$ is the reduction potential of the acceptor (viologen or pyridinium), $E_{(0,0)}$ is the singlet/triplet excited-state energy of acridine (singlet and triplet energies are 3.26 and 1.95 eV, respectively),[33] ϵ_s is the dielectric constant of the solvent used, r_D and r_A are the radii of the donor and acceptor molecules, and d_{cc} is the center-to-center distance between the ions. The values of r_D, r_A, and d_{cc} were estimated using a computer modeling program.[34] The changes in free energy values calculated for the electron transfer (ΔG_{el}) from the singlet excited state of acridine to viologen are found to be −1.24 and −1.27 eV in methanol and water, respectively. For the pyridinium systems, relatively lower change in free energy values were observed (−0.36 and −0.40 eV in methanol and water, respectively).[30] Similarly for the electron transfer from the triplet excited state of acridine to the viologen moiety, ΔG_{el} values are calculated to be 0.07 and 0.04 eV in methanol and water, respectively.

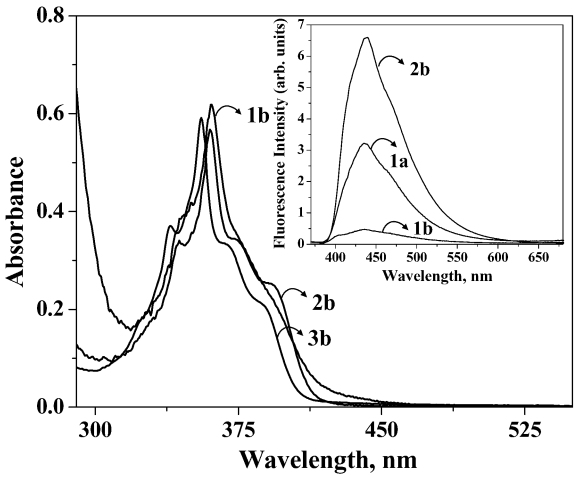

Figure 3. Absorption spectra of **1b** (6.8×10^{-5} M), **2b** (6.6×10^{-5} M), and *o*-tolylacridine (**3b,** 6.4×10^{-5} M) in water. The inset shows the fluorescence emission spectra of **2b** (1.3×10^{-5} M), **1a** (1×10^{-5} M), and **1b** (1.2×10^{-5} M) in water. Emission spectra of **1a** and **1b** are expanded by a factor of 20 for clarity. Excitation wavelength, 355 nm.

TABLE 1: Absorption and Fluorescence Characteristics of the Tolylacridine Derivatives[a]

	absorption		emission			
	λ_{max}, nm (ϵ, M^{-1} cm^{-1})		$10^2\Phi_f$[b]		τ, ns[c]	
compd	methanol	water	methanol	water	methanol	water
1a	359 (11300)	359 (12100)	0.8	0.60	1.7	5.4
1b	361 (9000)	361 (9100)	0.05	0.08	0.4	0.4
	585 (2250)				1.2	10.6
2a	359 (10750)	359 (10300)	3.8	26	1.1	3.9
2b	361 (9150)	360 (8550)	3.2	32	2.9	8.5
3b	356 (10450)	356 (9200)	5.8[d]	55.0	0.91	7.8

[a] Average of more than two experiments. [b] Fluorescence quantum yields are calculated using 9-aminoacridine as standard (Φ_f = 0.99);[16] error ca. ±5%. [c] Picosecond time-resolved fluorescence studies showed the existence of a short-lifetime species (τ < 50 ps) in the case of viologen linked acridines which could not be satisfactorily resolved within the instrument time scale. For details see the Supporting Information. [d] Fluorescence quantum yield and lifetime of *p*-tolylacridine (**3a**) in methanol are 0.059 and 0.74 ns, respectively.

Results and Discussion

Absorption and Fluorescence Emission Properties. Figure 3 shows the absorption spectra of the *o*-tolylacridine derivatives **1b**, **2b**, and **3b** in water. Similar spectra were obtained in the case of the *p*-tolylacridine derivatives **1a, 2a**, and **3a**. The absorption spectra of both the viologen and pyridinium linked tolylacridines **1a,b** and **2a,b** can be best described as the sum of the absorption bands of the individual units contained in them. However, a small red shift of around 3−5 nm was observed in the absorption maxima of the viologen and pyridinium linked tolylacridines when compared to those of the model acridine derivatives. There is no evidence for any ground-state charge-transfer interactions existing between the acridine and viologen/pyridinium moieties in these systems in water. Table 1 summarizes the absorption properties of the viologen and pyridinium linked tolylacridines in water and methanol. The viologen linked *o*-tolylacridine derivative **1b** in dry methanol,

on the other hand, unusually exhibited a broad and structureless absorption at around 585 nm with time, in addition to the absorption due to the acridine chromophore at 361 nm. This broad band decreased with increasing temperature and solvent viscosity and was not observed in acidic methanol solution. We tentatively assign this absorption to the existence of ground-state charge-transfer interaction between the viologen and acridine moieties in **1b**. By following the change in absorption of the acridine chromophore with pH, the pK_a values were determined and are found to be 4.9 and 3.5 for **1a** and **1b**, respectively. The comparison of pK_a values indicates that **1b** is more acidic than **1a** and further supports the presence of effective interactions between the acridine and viologen chromophores in the case of the *ortho*-derivative **1b**.

The inset of Figure 3 shows the fluorescence emission spectra of the viologen linked tolylacridines **1a** and **1b** and the pyridinium linked tolylacridine **2b** in water. The fluorescence properties, including the lifetimes of these compounds in water and methanol, are summarized in Table 1. The fluorescence yields of **1a** and **1b** were found to be very low when compared to those of the pyridinium linked derivatives **2a,b** and the model tolylacridines **3a,b**. For example, the pyridinium linked *o*-tolylacridine **2b** exhibited a fluorescence quantum yield of 0.32 in water, whereas the viologen linked tolylacridine derivatives **1a** and **1b** exhibited much lower quantum yields of 0.006 and 0.0008, respectively, indicating thereby that the fluorescence of the acridine unit is efficiently quenched by the viologen moiety in these systems. Furthermore, the quantum yields of **1a** in water and methanol were nearly 6 times higher than that of **1b**, suggesting an efficient quenching in the later case because of close proximity of the interacting units. In contrast, a reverse order was observed in the case of the pyridinium linked derivatives, where the *para*-derivative **2a** exhibited lower quantum yields of flourescence than that of the *otho*-derivative **2b** (Table 1). This observation reveals that the viologen moiety in the *ortho*-position undergoes a more efficient interaction with the acridine chromophore than that of the *ortho*-pyridinium moiety.

Nanosecond time-resolved fluorescence studies show that the *para*-viologen linked tolylacridine derivative **1a** and the pyridinium linked derivatives **2a** and **2b** exhibit single-exponential decay in both methanol and water (Table 1). In contrast, the *ortho*-viologen linked tolylacridine **1b** exhibited biexponential fluorescence decay in these solvents. These observations establish that **1a, 2a**, and **2b** exist as single conformers, whereas **1b** exists in two conformations in which the viologen moiety has different orientations with respect to the acridine plane. In one of the conformations, the viologen moiety lies above the acridine plane (folded conformation), wherein considerable spatial interactions exist between the two interacting units. In another conformer, the viologen is away from the acridine chromophore (extended conformation), where there is less chance for the existence of spatial interactions between the donor and acceptor moieties.[18]

Cyclic Voltammetry Studies. Figure 4 shows the cyclic voltammograms of **1b** and **2b** in acetonitrile. Under similar conditions, the oxidation of *o*-tolylacridine (**3b**) was observed to occur irreversibly at a half-wave potential of 1.6 V (vs SCE). Of the three reductions exhibited by the *ortho*-viologen linked tolylacridine derivative **1b** (Figure 4A), the first two, at the half-wave potentials −0.35 and −0.80 V, were found to be reversible while the reduction at the half-wave potential −1.54 V was observed to be irreversible. On the basis of literature evidence,[29] we assign the former two reductions to the viologen moiety

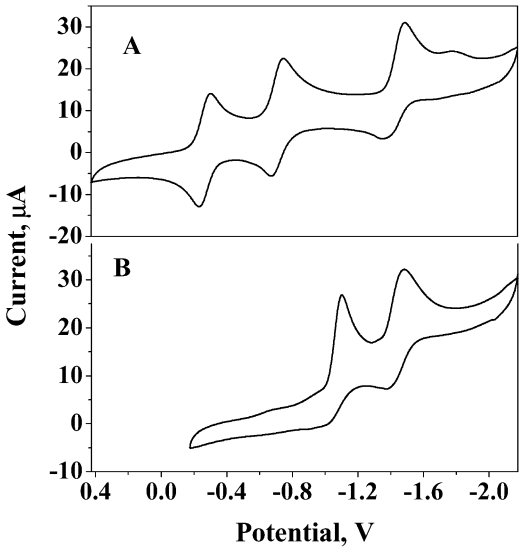

Figure 4. Cyclic voltammograms of (A) **1b** and (B) **2b** in acetonitrile showing the reduction peaks.

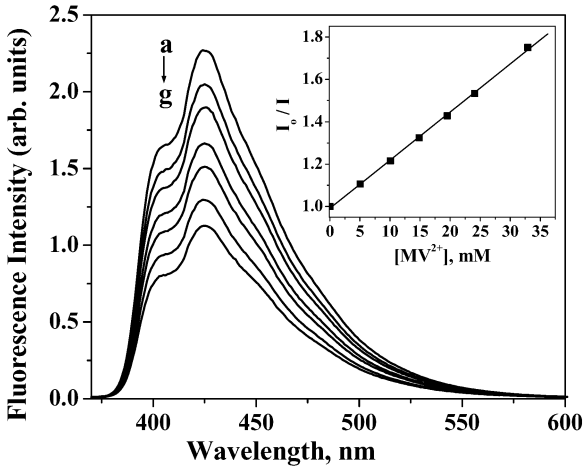

Figure 5. Effect of MV^{2+} concentration on the fluorescence emission spectra of *o*-tolylacridine (**3b**, 2.9×10^{-5} M) in methanol. [MV^{2+}]: (a) 0; (b) 5.1; (c) 10; (d) 14.8; (e) 24.1; (f) 32.9; (g) 41.3 mM. Inset shows the Stern−Volmer plot for the quenching of **3b** with MV^{2+}. Excitation wavelength, 355 nm.

whereas the third reduction could be attributed to the acridine chromophore. Similarly, the *para*-derivative **1a** showed three reduction waves in the voltammogram with no significant shifts, when compared to **1b**. The pyridinium linked tolylacridine derivative **2b**, on the other hand, showed only two reduction waves appearing at the half-wave potentials −1.15 and −1.53 V (Figure 4B). These reduction waves can be assigned to the reduction of the pyridinium and acridine moieties, respectively. Similar observations were made in the case of the *para*-pyridinium linked tolylacridine **2a**. The observation of similar redox potential values for the acridine chromophore in tolylacridines (**3a,b**), the viologen linked derivatives **1a,b**, and the pyridinium linked derivatives **2a,b** indicates that no ground-state interaction exists between the acridine chromophore and the acceptor moiety in these systems.

Electron-Transfer Studies. The intermolecular photoinduced electron-transfer reactions between tolylacridines (**3a,b)** and methyl viologen (MV^{2+}**)** were investigated by a fluorescence technique. Figure 5 shows the effect of the concentration of MV^{2+} on the fluorescence emission spectrum of **3b** in methanol, and the inset of Figure 5 shows the corresponding Stern−Volmer

TABLE 2: DNA Binding Constants (K), Intramolecular Electron Transfer Rate Constants (k_{ET}), Sums of Rate Constants of Singlet Excited State Deactivation (k_{SI}), and Rate Constants of Quenching by DNA (k_{DNA}) of Viologen/Pyridinium Linked Tolylacridine Derivatives 1a,b and 2a,b[a]

compd	K,[b] M^{-1}	k_{ET}, s^{-1}	k_{SI},[c] s^{-1}	k_{DNA}, s^{-1}
1a	$(1 \pm 0.1) \times 10^5$	1.16×10^{10}	1.17×10^{10}	7×10^9
1b	nb[d]	8.8×10^{10}	8.81×10^{10}	nb[d]
2a	$(3.3 \pm 0.2) \times 10^5$	1.4×10^8	2.7×10^8	3×10^9
2b	nb[d]	0.9×10^8	2.2×10^8	nb[d]

[a] Average of more than two experiments. [b] Calculated on the basis of fluorimetric titration of the probe against calf thymus DNA in 10 mM phosphate buffer (pH 8) containing 50 mM NaCl. K for **1a** at 100 mM NaCl is 4.9×10^4 M^{-1}. [c] $k_{SI} = k_d + k_{ET}$ is the sum of radiative and nonradiative rate constants for deactivation of the acridine singlet excited state (k_d) and the intramolecular electron-transfer rate constant (k_{ET}). [d] nb = exhibited negligible binding with DNA.

plot. The quenching rate constants were calculated by employing the Stern−Volmer equation (eq 2)

$$I_0/I = 1 + K_{sv}[Q] \tag{2}$$

and

$$K_{sv} = k_q \tau_0 \tag{3}$$

where I_0 and I are the fluorescence intensities in the absence and presence of the quencher (Q), K_{sv} is the Stern−Volmer constant, τ_0 is the fluorescence lifetime of the tolylacridine in the absence of quencher, and k_q is the quenching rate constant. On the basis of fluorescence titration data, the calculated bimolecular fluorescence quenching rate constants for **3a** and **3b** are found to be 2.51×10^{10} and 2.54×10^{10} M^{-1} s^{-1}, respectively. The observed high fluorescence quenching rate constants and the calculated change in free energy ($\Delta G = -1.24$ eV in methanol) for the electron transfer from the singlet excited state of tolylacridine to MV^{2+} indicate that both these acridine derivatives (**3a** and **3b)** are capable of donating electrons to the viologen moiety very efficiently.

In the case of the covalently linked systems **1a,b** and **2a,b**, an estimate of the intramolecular electron-transfer rate constants (k_{ET}) can be made on the basis of the fluorescence quantum yields and the lifetime of the corresponding model compound and using eq 4,

$$k_{ET} = [(\Phi_{ref}/\Phi) - 1]/\tau_{ref} \tag{4}$$

where k_{ET} represents the intramolecular electron-transfer rate constant, Φ_{ref} and Φ are the relative fluorescence quantum yields of the corresponding model compound and the acceptor linked tolylacridine, respectively, and τ_{ref} is the fluorescence lifetime of the model compound. The intramolecular electron-transfer rate constants for the viologen and pyridinium linked tolylacridine derivatives **1a,b** and **2a,b** in water were estimated and are summarized in Table 2.

As shown in Table 2, the *ortho*-derivative **1b** exhibits higher electron-transfer rate constants in both methanol and water ($k_{ET} = 1.3 \times 10^{11}$ and 8.8×10^{10} s^{-1}), when compared to those of the *para*-derivative **1a** ($k_{ET} = 6.9 \times 10^{10}$ and 1.16×10^{10} s^{-1}). This can be attributed to the existence of strong through-space interactions between the acridine and viologen units in **1b**, whereas no such possibility exists in the case of **1a**. The pyridinium linked tolylacridine derivatives **2a** ($k_{ET} = 5.8 \times 10^8$ and 1.4×10^8 s^{-1} in methanol and water) and **2b** ($k_{ET} = 9 \times 10^8$ and 0.9×10^8 s^{-1}), on the other hand, showed nearly 2−3 orders lower electron-transfer rate constants, when compared

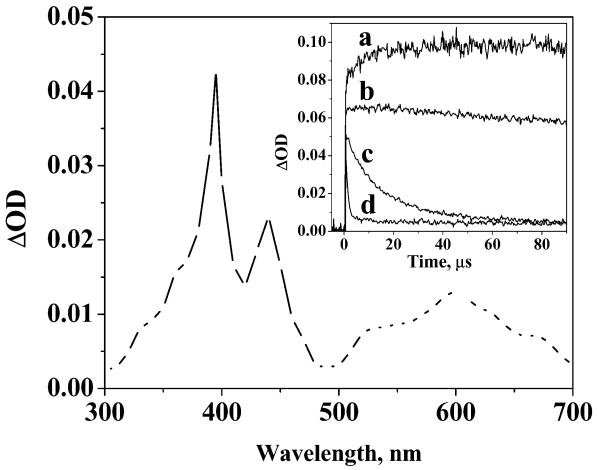

Figure 6. Transient absorption spectrum obtained immediately after 355 nm laser excitation (pulse width 20 ns) of an argon saturated solution of *o*-tolylacridine (**3b**, 5.1×10^{-5} M) in the presence of MV^{2+} (1.3 mM). Inset shows the growth of the reduced methyl viologen radical cation at 395 nm under (a) argon saturated and (b) air saturated conditions and the decay of the acridine triplet excited state at 440 nm under (c) argon saturated and (d) air saturated conditions.

to **1a** and **1b**. This fact was further substantiated by the observation of lower change in free energy values for the pyridinium systems ($\Delta G_{el} = -0.36$ and -0.40 eV, in methanol and water, respectively), when compared to the viologen linked derivatives ($\Delta G_{el} = -1.24$ eV and -1.27 eV, in methanol and water, respectively). These observations indicate that the pyridinium moiety is less efficient in oxidizing the acridine chromophore when compared to the viologen and that the spacer group in these systems exhibits a control over the rate of electron-transfer reactions by positioning the donor and acceptor moieties at different distances.

Laser Flash Photolysis Studies. Laser flash photolysis experiments were carried out under different conditions to characterize the transient intermediates involved in these systems. For example, Figure 6 shows the transient absorption spectrum obtained immediately after laser excitation (355 nm, pulse width 20 ns) of *o*-tolylacridine (**3b)** in methanol and in the presence of methyl viologen (MV^{2+}; 1.3 mM). On the basis of quenching experiments with molecular oxygen, the transient species with absorption maxima at 440 nm could be assigned to the triplet excited state of **3b**. As per the literature evidence,[35] the other transient with two absorption maxima at 395 and 610 nm could be assigned to the reduced methyl viologen radical cation formed by the electron-transfer reaction from **3b** to MV^{2+}. Interestingly, the reduced methyl viologen radical cation formed is found to be quite stable in methanol under argon atmosphere. The inset of Figure 6 shows the decay of the acridine triplet and the growth of the methyl viologen radical cation, under argon saturated and air saturated conditions.

The reduced methyl viologen radical cation can form by electron-transfer reaction, from either the singlet or the triplet excited states of acridine to MV^{2+}. To estimate the contributions of both these excited states, we have examined the electron-transfer reactions as a function of MV^{2+} concentration. When the concentration of MV^{2+} used was very low ($\sim 10^{-5}$ M), the growth of the methyl viologen radical cation was found to be concomitant with the decay of the triplet excited state of acridine. Its formation by quenching of the singlet excited state would be <5% at these concentrations. At higher concentrations of MV^{2+}, the growth of the methyl viologen radical cation became clearly biexponential with a sudden growth immediately after the laser pulse followed by a slow growth. Under air

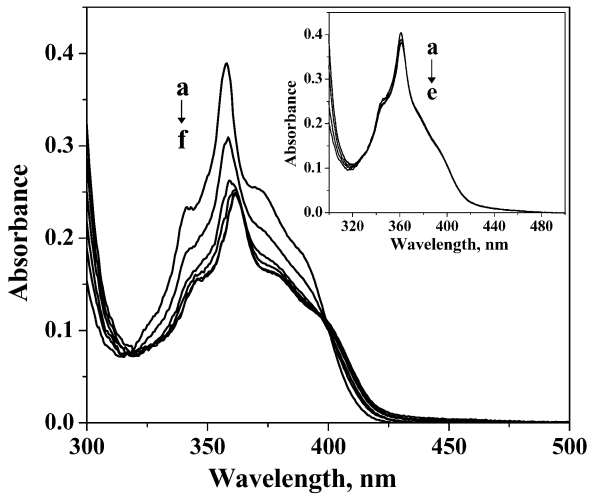

Figure 7. Absorption spectra of **1a** (3.2×10^{-5} M) in the presence of CT DNA in 10 mM phosphate buffer (pH 8) containing 50 mM NaCl. [DNA]: (a) 0; (b) 0.07; (c) 0.14; (d) 0.20; (e) 0.33; (f) 0.44 mM. Inset shows the absorption spectra of **1b** (4.4×10^{-5} M) in the presence of CT DNA under analogous conditions. [DNA]: (a) 0; (b) 0.14; (c) 0.38; (d) 0.60; (e) 1 mM.

saturated conditions, on the other hand, the triplet excited state of acridine was quenched by molecular oxygen, and therefore, we observed negligible formation of the reduced methyl viologen radical cation (inset of Figure 6).

Direct 355 nm laser excitation of the viologen linked tolylacridines **1a** and **1b** in water or methanol did not show any transients. However, in the presence of an external donor such as guanosine, both these derivatives showed transients corresponding to the reduced methyl viologen radical cation. This observation can be attributed to the existence of a fast charge recombination reaction in these covalently linked systems and the presence of sacrificial donors found to stabilize the charge-separated species. Interestingly, the laser flash studies of **1a** and **1b** in the presence of calf thymus DNA showed contrasting results. Of these two derivatives, only the *para*-derivative **1a**, which showed strong affinity for DNA (see section DNA Binding Studies), exhibited the transient formation corresponding to the reduced methyl viologen radical cation in the presence of DNA. These results reveal that effective binding of the viologen linked tolylacridines to DNA is very essential for the oxidation of DNA and also for the generation of charge-separated species.

DNA Binding Studies. To find out how the substitution affects the DNA intercalating and groove binding properties of the acridine and viologen chromophores, we have studied the DNA binding properties of the viologen and pyridinium linked tolylacridines **1a,b** and **2a,b** in 10 mM phosphate buffer using absorption and fluorescence techniques. Figure 7 shows the change in absorption spectrum of the viologen linked *p*-tolylacridine **1a** with increasing in concentration of DNA. Upon increasing DNA concentration, the absorption spectra corresponding to the acridine chromophore showed strong hypochromism (~40%) as well as a 3 nm bathochromic shift, suggesting the interaction of the acridine moiety with DNA by intercalation, whereas, in the case of the *ortho*-derivative **1b**, the absorption spectra showed negligible changes with the increase in DNA concentration, as shown in the inset of Figure 7. Similar observations were made in the case of the pyridinium linked tolylacridine derivatives **2a** and **2b**, where only the *para*-derivative **2a** undergoes interaction with DNA, while the *otho*-derivative **2b** showed negligible affinity for DNA.

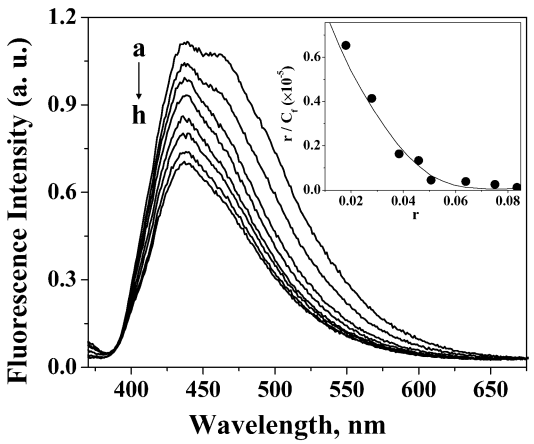

Figure 8. Fluorescence emission spectra of **1a** (3.2×10^{-5} M) in the presence of CT DNA in 10 mM phosphate buffer (pH 8) containing 50 mM NaCl. [DNA]: (a) 0; (b) 0.07; (c) 0.14; (d) 0.33; (e) 0.44; (f) 0.64; (g) 0.82; (h) 1.4 mM. Inset shows the Scatchard plot for the binding of **1a** to CT DNA. Excitation wavelength, 355 nm.

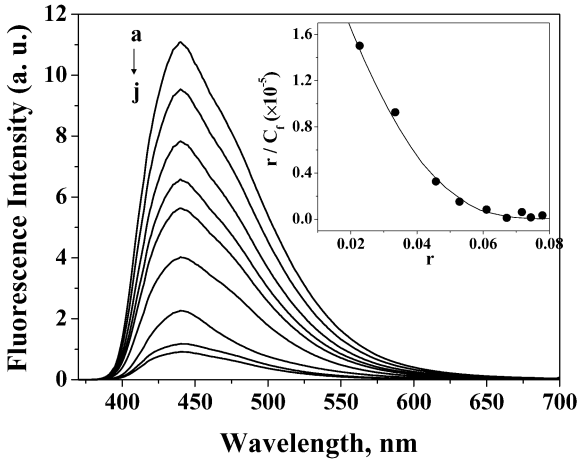

Figure 9. Fluorescence emission spectra of **2a** (3.7×10^{-5} M) in the presence of CT DNA in 10 mM phosphate buffer (pH 8) containing 50 mM NaCl. [DNA]: (a) 0; (b) 0.07; (c) 0.14; (d) 0.20; (e) 0.26; (f) 0.38; (g) 0.5; (h) 0.69; (i) 1.22; (j) 1.5 mM. Inset shows the Scatchard plot for the binding of **2a** to CT DNA. Excitation wavelength, 355 nm.

Furthermore, the interaction of these bifunctional molecules with DNA was studied using the fluorescence technique. Figures 8 and 9 show the change in fluorescence emission spectra of the viologen linked *p*-tolylacridine derivative **1a** and the corresponding pyridinium derivative **2a**, respectively, with increasing concentration of DNA.

Only the *p*-tolylacridine derivatives **1a** and **2a** exhibited strong interaction with DNA, while the fluorescence emission properties of the *ortho*-derivatives **1b** and **2b** remained unchanged in the presence of DNA, indicating thereby the negligible binding of the *ortho*-derivatives with DNA. The association constant (K) of the complex formed between the *para*-derivatives **1a** and **2a** and DNA was calculated according to the method of McGhee and von Hippel and using the data points of the Scatchard plot (insets of Figures 8 and 9).[22−24] The pyridinium linked derivative **2a** exhibited a greater association constant ($K = (3.3 \pm 0.2) \times 10^5$ M^{-1}) when compared to that of the viologen linked derivative **1a** ($K = (1 \pm 0.1) \times 10^5$ M^{-1}), indicating thereby that even the remote steric factors of the substituents perturb the intercalating interactions of the acridine moiety with DNA.

On the basis of limiting fluorescence intensity (under conditions where >99% of the substrate is bound to DNA), the rate

constant for the static quenching of the singlet excited state of the acridine chromophore in these molecules by DNA (k_{DNA}) was evaluated using eq 5,

$$I_0/I = 1 + k_{DNA}/k_{SI} \quad (5)$$

where I_0 and I are the fluorescence intensities in the absence and presence of DNA and k_{SI} is the sum of the rate constants ($k_d + k_{ET}$) of the singlet excited-state deactivation.[16] The k_{DNA} values obtained for these derivatives are summarized in Table 2. The static quenching rate constant (k_{DNA}) for **1a** was found to be 7×10^9 s^{-1}, whereas a lower value of 3×10^9 s^{-1} was observed for the pyridinium linked derivative **2a**. This observation indicates that the viologen linked *p*-tolylacridine derivative **1a**, though, binds less efficiently but is more efficient in oxidizing the DNA bases when compared to the corresponding pyridinium derivative **2a**.

The calculated change in free energy value for the electron-transfer reactions using oxidation potentials of DNA bases[36] and the reduction potential of acridine ($\Delta G = -0.64$, -0.51, -0.33, and -0.23 eV for guanine, adenine, cytosine, and thymine, respectively) shows that all DNA bases can quench the fluorescence of the acridine moiety by an electron-transfer mechanism. The extent of fluorescence quenching offered by DNA depends on the type of interaction of these molecules undergo with DNA. In the case of the *ortho*-derivatives **1b** and **2b**, the steric effects offered by the substitutent groups prevent the interaction of the acridine moiety with DNA. These results suggest that the rotation around the acridine and phenyl units is crucial in the process of intercalation of the acridine moiety into the DNA core. In the case of the *p*-tolyl derivatives **1a** and **2a**, the rotation around these interacting units is facile when compared to that of the sterically crowded *o*-tolyl derivatives, and hence intercalation of the acridine chromophore was observed only in the case of the *para*-derivatives.

Conclusion

In summary, the absorption and cyclic voltammetry studies of the viologen and pyridinium linked tolylacridines **1a,b** and **2a,b** show that there are no ground state interactions existing between the acridine and acceptor moieties. The fluorescence quantum yields of the viologen linked tolylacridines were found to be lower when compared to those of the pyridinium linked and unsubstituted tolylacridine derivatives, suggesting thereby that the fluorescence of the acridine chromophore is efficiently quenched by the viologen moiety in these systems. Calculated free energy changes and bimolecular fluorescence quenching rate constants indicate that the photoinduced electron transfer is the predominant nonradiative pathway in these systems. The intramolecular electron-transfer rate is found to be more efficient in the case of the viologen linked *ortho*-derivative **1b** when compared to the *para*-derivative **1a**, indicating thereby the existence of strong through-space interactions between the acridine and viologen moieties in the former case. DNA binding studies showed that only the *para*-derivatives **1a** and **2a** undergo efficient interaction with DNA while the corresponding *o*-tolylacridine derivatives exhibited negligible affinity for DNA. The static quenching rate constants by DNA (k_{DNA}) indicate that the viologen linked *p*-tolylacridine derivative **1a** is a better DNA oxidizing agent when compared to the corresponding pyridinium derivative **2a**. These results demonstrate that the tolyl spacer group constitutes an interesting variation that controls the photophysical and DNA binding properties of these molecules. Furthermore, the viologen linked *p*-tolylacrdine derivative **1a**, which exhibited greater affinity for DNA and oxidizes DNA very efficiently, can have potential use as a DNA probe and as a DNA cleaving agent that functions through the cosensitization mechanism.

Acknowledgment. We are grateful to the Council of Scientific and Industrial Research (CSIR) and Department of Science and Technology, Government of India, for the financial support of the work. This is contribution no. RRLT-PPD(PRU)-159 from the Regional Research Laboratory, Trivandrum.

Supporting Information Available: Fluorescence decay profile of **1a**. This material is available free of charge via the Internet at http://pubs.acs.org.

References and Notes

(1) Bischofberger, N.; Shea, R. G. In *Nucleic Acid Targeted Drug Design*; Propst, C. L., Perun, T. J., Eds.; Dekker: New York, 1992; p 579.
(2) Tidd, D. M. In *Molecular Aspects of Anticancer Drug−DNA Interactions, Vol. 1*; Neidle, S., Waring, M., Eds.; CRC: Boca Raton, FL, 1993; p 272.
(3) Tullius, T. In *Metal-DNA Chemistry*; ACS Symposium Series 402; American Chemical Society: Washington, DC, 1989.
(4) Barton, J. K. In *Bioinorganic Chemistry*; University Science Books: Mill Valley, CA, 1994; p 455.
(5) Wilson, W. D.; Jones, R. L. In *Intercalator Chemistry*; Whittingham, M. S., Jacobson, A. J., Eds.; Academic Press: New York, 1982; p 445.
(6) Pullman, B.; Jortner, J. *Molecular Basis of Specificity in Nucleic Acid-Drug Interactions*, Vol. 1; CRC: Ann Arbor, MI, 1993.
(7) Armitage, B.; Yu, C.; Devadoss, C.; Schuster, G. B. *J. Am. Chem. Soc*. **1994**, *116*, 9847.
(8) Nielsen, P. E. *Bioconjugate Chem*. **1991**, *2*, 1.
(9) Schuster, G. B. *Acc. Chem. Res.* **2000**, *33*, 253.
(10) Giese, B. *Acc. Chem. Res.* **2000**, *33*, 631.
(11) Kumar, C. V.; Asuncion, E. H. *J. Am. Chem. Soc.* **1993**, *115*, 8547.
(12) Nakatani, K.; Sando, S.; Saito, I. *J. Am. Chem. Soc.* **2000**, *122*, 2172.
(13) Takenaka, S.; Ihara, T.; Takagi, M. *Chem. Lett.* **1992**, 1.
(14) Armitage, B. *Chem. Rev.* **1998**, *98*, 1171 and references therein.
(15) Dunn, D. A.; Lin, V. H.; Kochevar, I. E. *Biochemistry* **1992**, *31*, 11620.
(16) Rogers, J. E.; Le, T. P.; Kelly, L. A. *Photochem. Photobiol*. **2001**, *71*, 223.
(17) Le, T. P.; Rogers, J. E.; Kelly, L. A. *J. Phys. Chem. A* **2000,** *104*, 6778.
(18) Eldho, N. V.; Joseph, J.; Ramaiah, D. *Chem. Lett.* **2001**, 438.
(19) Junjappa, H.; Saxena, M. K.; Ramaiah, D.; Loharay, B. B.; Rath, N. P.; George, M. V. *J. Org. Chem*. **1998**, *63*, 9801.
(20) Sajimon, M. C.; Ramaiah, D.; Thomas, K. G.; George, M. V. *J. Org. Chem.* **2001,** *66*, 3182.
(21) Weber, G.; Teale, F. W. J. *Trans. Faraday Soc.* **1957**, *53*, 646.
(22) Scatchard, G. *Ann. N. Y. Acad. Sci.* **1949**, *51*, 660.
(23) McGhee, J. D.; von Hippel, P. H. *J. Mol. Biol*. **1974**, *86*, 469.
(24) Adam, W.; Cadet, J.; Dall'Acqua, F.; Epe, B.; Ramaiah, D.; Saha-Möller, C. R. *Angew. Chem., Int. Ed. Engl*. **1995**, *34*, 107.
(25) Baguley, B. C.; Falkenhang, E.-M. *Nucleic Acids Res.* **1978**, *5*, 101.
(26) Zhao, T.-G.; Shen, T.; Xu, H.-J. *J. Photochem. Photobiol. A: Chem.* **1990**, *52*, 4753.
(27) Bernthsen, A. *Justus Liebigs Ann. Chem.* **1884**, *224*, 1.
(28) Jonker, S. A.; Ariese, F.; Verhoeven, J. W. *Recl. Trav. Chim. Pays-Bas* **1989**, *108*, 109.
(29) Ledwith, A. *Acc. Chem. Res.* **1972**, *5*, 133.
(30) Mann, C. K.; Barnes, K. K. *Electrochemical Reactions in Nonaqueous Systems*; Marcel Dekker: New York, 1970; p 324.
(31) Rehm, D.; Weller, A. *Ber. Bunsen-Ges. Phys. Chem.* **1969**, *73*, 834.
(32) Weller, A. *Z. Phys. Chem.* **1982**, *133*, 93.
(33) Murov, S. L.; Carmichael, I.; Hug, G. L. *Handbook of Photochemistry*, 2nd ed.; Marcel Dekker: New York, 1993.
(34) Titan software version 1 from Wavefunction, Inc., 18401 Von Karman, Suite 370, Irvine, CA 92612.
(35) Watanabe, T.; Honda, K. *J. Phys. Chem*. **1982**, *86*, 2617.
(36) Steenken, S.; Jovanovich, S. V. *J. Am. Chem. Soc*. **1997**, *119*, 617.